The Iranian Journal of Mechanical Engineering Transactions of ISME
Journal homepage: https://jmee.isme.ir/
Vol. 26, No. 1, 2025, pp. 114-129

Research Paper

DOI: https://doi.org/10.30506/jmee.2024.2037541.1352

A Comparison of Corrosion Behavior of Coarse and Ultrafine Grain Commercially Pure Titanium in Simulated Body Fluid

Reza Naseri[*]
Assistant Professor

Hasan Heirani[†]
Assistant Professor

Mohammad Hossein Mozaffari[‡]
Assistant Professor

Reza Babaei Spouei[§]
PhD

Equal channel angular pressing (ECAP) is one of the most effective processes for the production of metals with ultra-fine grains (UFG) and nano-crystalline (NC) structures. Commercially pure titanium (CP-Ti) known for its excellent biocompatibility, has high potential for use in medical applications as an implant material. The low static and dynamic strength of CP-Ti are weaknesses of this material that can be remedied by applying ECAP to create UFG microstructures. One of the most important parameters in choosing a material for implantation is its corrosion resistance in human body plasma. In this study, the corrosion behavior of primary coarse grained (CG) and ultra-fine grained CP-Ti produced by ECAP was investigated and compared in simulated body fluid (SBF) through the extraction of the TAFEL curve. The results demonstrated that the corrosion resistance of CP-Ti in the UFG state was improved by seven times compared to the initial CG state. This improvement can be attributed to increased passivation ability resulting from rapid mechanical formation of a stable and strong passive oxide film of TiO2 on UFG surface of CP-Ti relative to CG.

Keywords: Commercially pure titanium, ECAP, Ultra-fine grains, Corrosion resistance, Simulated body fluid

[*]Corresponding author, Assistant Professor, Department of Mechanical Engineering, National University of Skills (NUS), Tehran, Iran,
PhD, Department of Mechanical Engineering, Faculty of Engineering, Ferdowsi University of Mashhad, Mashhad, Iran, rnaseri@tvu.ac.ir
[†]Assistant Professor, Department of Mechanical Engineering, Faculty of Engineering, Bozorgmehr University of Qaenat, Qaen, Iran, heirani@buqaen.ac.ir
[‡]Assistant Professor, Department of Mechanical Engineering, National University of Skills (NUS), Tehran, Iran, mhmozaffari@tvu.ac.ir
§ PhD, Department of Mechanicl Engineering, Tarbiat Modares University, Tehran, Iran, r.babaei@modares.ac.ir

Received: 2024/08/04, Revised: 2024/09/23, Accepted: 2024/12/04

1 Introduction

Today, titanium and its alloys are widely used in various industries. Positive properties such as low density, high specific strength, low elastic modulus, excellent corrosion resistance, good biocompatibility, durability at high temperatures, acceptable casting capability and good welding capability have made titanium being one of the most popular and widely used metals in the automotive and aerospace industries and in biomedical industry for orthopedic and dental implants [1-4]. The Ti-6Al-4V titanium alloy is one of the most common and widely used titanium alloys which has a significant percentage of aluminum and vanadium elements. It has been proven that these elements are toxic similar to other alloying elements such as nickel, cobalt and chromium. Long-term ion releasine can lead to neurological diseases, Alzheimer, cancer, dermatitis, bone softening and other health issues [1, 3, 5]. Therefore, the demand for the replacement of commercially pure titanium (CP-Ti) for titanium alloys in biomedical applications has increased due to its lower alloying elements and lower cost [3, 6]. The main disadvantage of CP-Ti is its low mechanical strength compared to titanium alloys such as Ti-6Al-4V, hence CP-Ti is not widely utilized in the industry [1].

Among the many methods of severe plastic deformation (SPD), equal channel angular pressing (ECAP) is one of the most effective and widely used techniques [7]. Using this technique, large scale metallic work-pieces with relatively homogeneous ultra-fine grain (UFG) and nano-crystalline (NC) structures with high-angle grain boundaries (HAGBs) can be produced [7, 8]. In this method, by applying high strains on the coarse grain (CG) metal and creating a high density of dislocations and rearranging them to form the new grain boundaries, grains with size in the range of micrometers or nanometers are created, and low-angle grain boundaries (LAGBs) develop to HAGBs. Therefore, the static and dynamic strength of the material increases sharply according to Hall-Petch theory [7, 9].

Biocompatibility is one of the most important parameters in using a material in medical applications especially as an implant material. The study of the biocompatibility of UFG CP-Ti and bone cohesion due to surface topology, has been extensively performed, all of which have shown improved biocompatibility, improved bone cohesion, better cell adhesion and cell proliferation in UFG than primary CG states. It has been proved that this can be related to the higher surface and grain boundary energy in UFG relative CG titanium and even Ti-6Al-4V alloy [10-16].

Corrosion resistance in the body environment affects on the biocompatibility of a material [10, 17]. In vitro investigations, simulated body fluid (SBF) or Hank's solution is used as a fluid similar to human body plasma for corrosion testing [18]. A review of the literatures has shown that few studies have been conducted on the comparison of the corrosion resistance of UFG with CG CP-Ti in the electrolyte of the SBF. All studies have shown that UFG CP-Ti has several times higher corrosion resistance than primary CG CP-Ti, and this is due to the formation of quicker passivation and strong oxide films of TiO_2 on the surface of the ultra-fine grain pure titanium [10, 16, 19-22].

In 2020, Dong et al. investigated the effect of NaCl and Ringer solution on CP-Ti and Ti-6Al-7Nb alloy titanium in both CG and UFG states. The results of the study showed that the corrosion behavior in UFG state is significantly improved compared to CG state [23]. In 2024, Chuvildeev et al. [24] investigated the corrosion-fatigue strength of the fine-grained near-α alloy Ti-5Al-2V in a 3% aqueous NaCl solution, as well as its resistance to hot salt corrosion. Cold rotary swaging was found to enhance the depth of intergranular corrosion defects, while recrystallization annealing improved the corrosion resistance of the Ti-5Al-2V titanium alloy. Maleki-Ghaleh et al. in 2014, using polarization and electrochemical impedance tests in a SBF environment at 37°C on UFG CP-Ti produced by ECAP, showed that corrosion resistance and biological behavior in UFG compared to CG state were remarkably improved [10]. Comparison

of the corrosion behavior of CG and UFG CP-Ti has been performed in different solutions. The effect of annealing on the corrosion behavior of UFG CP-Ti was investigated by Kim et al. in 2014 in 0.5 M H_2SO_4 solution using potentiodynamic polarization and weight loss methods. The results showed that annealing after introducing SPD can make a suitable combination of high strength and high corrosion resistance while maintaining an ultra-fine grain size [25]. Otadi et al. [26] employed a combination of techniques to enhance the corrosion performance of commercially pure titanium. These techniques included grain refinement through equal channel angular pressing, two-step anodization to create titanium oxide nanotube coatings, annealing at 450°C and 570°C, and immersion in simulated body fluid to form a hydroxyapatite film coating. The corrosion behavior was assessed using potentiodynamic polarization tests and electrochemical impedance spectroscopy. The results demonstrated that grain refinement and the successive surface modifications significantly influenced the corrosion performance. The effect of grain size and texture on the corrosion behavior of CP-Ti in SBF was investigated by Gurao et al. in 2013. The results proved that the optimal combination of microstructure and crystallographic texture leads to improved strength and higher corrosion resistance after applying the SPD process [27]. Zheng et al. in 2011, applied ECAP on CP-Ti and then created a hierarchical porous surface using sandblasting, acid etching, and alkali treatment techniques. Corrosion test of this material in SBF showed that there is no pitting corrosion in UFG CP-Ti with the modified surface and the corrosion rate was very low [28]. Mendes Filho et al. in 2010, subjected grade (2) CP-Ti to hot and cold ECAP and proved that there was no noticeable difference between the corrosion behavior of the initial annealed material and the ECAPed material in NaCl solution. In this study, the potentiodynamic polarization method was used for investigation of corrosion properties [19]. The effect of grain size and texture on the corrosion properties of CP-Ti was studied by Hoseini et al. in 2009 in NaCl aqueous solution. The investigation of corrosion behavior using electrochemical impedance spectroscopy demonstrated that corrosion resistance increases significantly with decreasing grain size [22]. Balakrishnan et al. in 2008, using the TAFEL extrapolation method, showed that the corrosion resistance of UFG Ti in SBF medium is ten times greater than CG-Ti. In this research, the ECAP method was utilized to achieve the UFG microstructure [21]. In 2024, Nair and Swaroop [29] investigated laser shock peening of the medical-grade Ti-6Al-7Nb titanium alloy without coating. They subsequently examined the role of the oxide layer formed and the microstructural changes related to biocorrosion in simulated body fluid. The results indicated that under the 6 GW/cm² condition, a high dislocation density, a significant fraction of high-angle grain boundaries, and a refined β phase present beneath the oxide layer serve as sites for passivation, contributing to enhanced anti-biocorrosion capabilities. Balyanov et al. in 2004 demonstrated that UFG alloy titanium by SPD processes has higher corrosion resistance than its initial state in acidic HCl and H_2SO_4 solutions. Rapid passivation of UFG Ti and impurity segregation to grain boundaries in CG were cited as reasons for the better corrosion behavior of UFG Ti than CG Ti [30]. In the latest research conducted by Fakhri et al. in 2024 [31], the fluoride-induced corrosion performance of UFG CP-Ti was investigated. The ultrafine titanium was produced by ECAP process combined with ultrasonic vibrations. The results demonstrated that a significant improvement in mechanical properties and corrosion behavior after applying U-ECAP. It was also observed that the film on the 3 passes ECAPed samples was denser and more uniform, and at least twice as thick as the non-ECAP samples.

It should be noted that very limited research has been done on the fundamental understanding of the effect of grain size and consequently grain refinement on the corrosion resistance of metal alloys. It is essentially emphasized that the effect of grain refinement is a very complicated phenomenon and generally active, passive and or active-passive responses have been observed in various materials in different media. It has been proven that other factors such as internal stresses and strains, the effects of precipitate size, texture type and or method of applying

processes can be more influential factors than grain size. However, generally has been found that grain refining increases the corrosion resistance of magnesium and titanium alloys. In the case of other materials, a permanent effect was not observed and grain refinement depending on the process of its creation and the corrosive medium, led to an increase or decrease in corrosion resistance. However, research has demonstrated that the main reason for the improvement of corrosion resistance in UFG metals depends on the improvement of the formation and adhesion of the passive film due to the increase in density of grain boundaries [32, 33].

A review of the literature has shown that few investigations were conducted on the corrosion behavior of UFG CP-Ti in the SBF. Most of this research has focused on applying hot/warm SPD processes on titanium and its alloys. In this study, by applying cold ECAP process at ambient temperature on grade (2) commercial pure titanium and creating an ultra-fine grain microstructure, TAFEL test method is used to evaluate and compare the corrosion resistance of this material in UFG and CG states in the SBF environment.

2 Material and experimental procedures

2.1 Materials

The specimen used in the present experiments was a bimetallic work-piece. Reducing the pressing force, improving the mechanical properties, increasing the homogeneity of the deformation and increasing the distribution uniformity of effective strain are the reasons for using bimetallic specimens [34-37]. Grade (2) commercially pure titanium rods were inserted as core material or billets into the aluminum 7075 casing with an interference fit. The schematic view and dimensions of the used bimetallic specimen are shown in Figure (1). Chemical composition of Grade (2) CP-Ti and Al-7075 obtained by emission spectrometry; are presented in Table (1).

In order to stabilize and homogenize the microstructure and eliminate the residual stresses, CP-Ti was annealed at 800 °C for one hour and then cooled in air and in a shut-off furnace [38, 39]. Al-7075 was also annealed at 415 °C for one hour and cooled in a shut-off furnace [34]. Using this heat treatment, an equiaxed and homogenous microstructure with an average coarse grain size of 55 μm for CP-Ti was achieved.

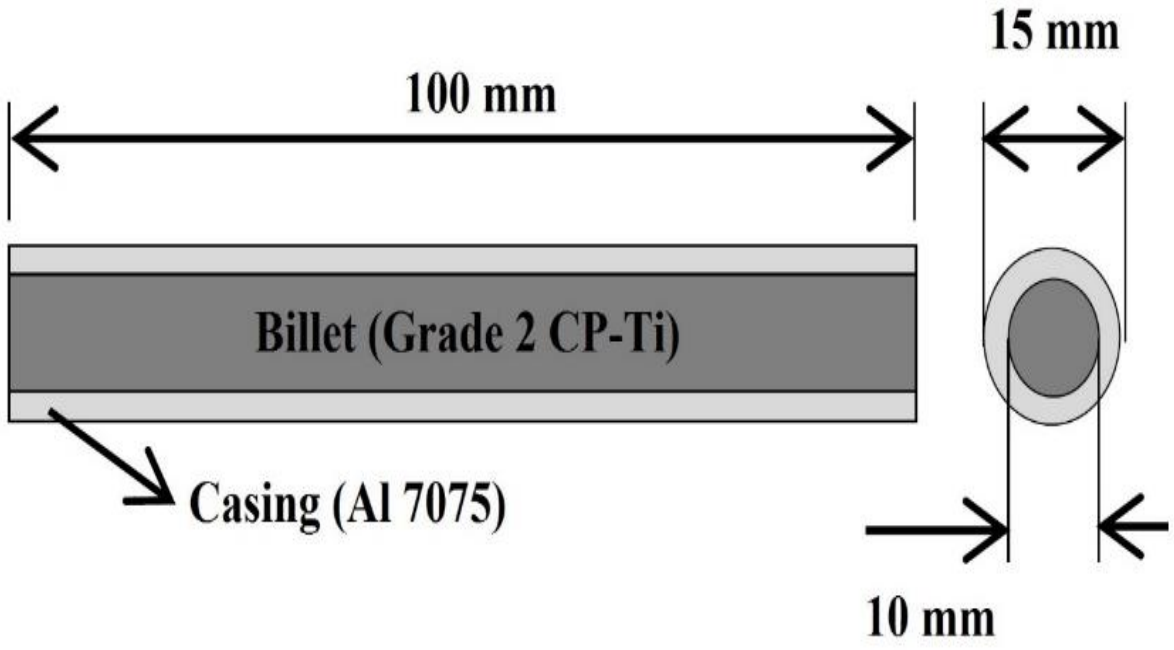

Figure 1 Schematic illustration and dimensions of the bimetallic rod specimen for ECAP

Table 1 Chemical composition of grade (2) CP-Ti and Al-7075 alloy (%wt)

Grade 2 CP-Ti	**Ti**	**Fe**	**C**	**N**	**H**	**O**		
	Base	0.02	0.02	0.03	0.001	0.06		
Al-7075	**Al**	**Zn**	**Mg**	**Cu**	**Fe**	**Si**	**Cr**	**Mn**
	Base	5.78	2.73	1.47	0.36	0.34	0.21	0.05

2. 2 ECAP process

The ECAP process was performed at room temperature using a hydraulic press with a nominal capacity of 60 tons and a ram speed of 9 mm/s. To conduct the ECAP, a die with channel circular cross-section channel with diameter of 15 mm, a channel angle of 135°, and a corner angle of 20° was used. In each separate pass, a strain about 0.46 was applied to the bimetallic specimen [7].

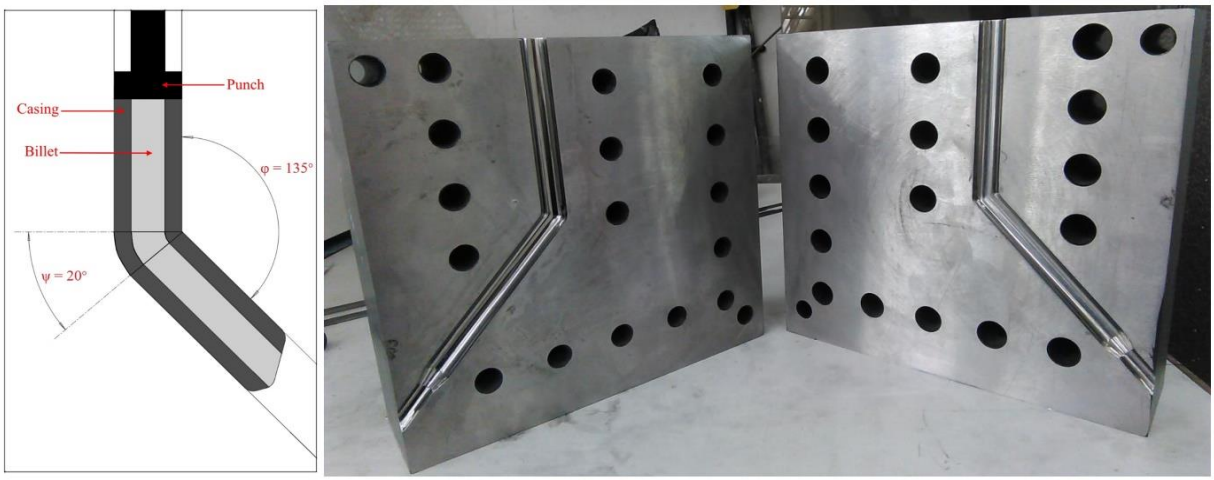

Figure 2 Schematic and real illustrations of ECAP die with bimetallic specimen including CP-Ti as billet and Al-7075 as casing

Figure 3 Bimetallic specimens, before and after 1 to 3 passes of ECAP

Figure (2) shows a schematic and real view of the used ECAP die. To reduce the friction force between specimens and die wall, a lubricant with the brand name of MOLYKOTE ® 1000 PASTE was utilized. Firstly, specimens were subjected to four passes in the route Bc by ECAP. This route was chosen because it leads to the rapid formation of homogeneous/equiaxed ultra-fine grain microstructure with high-angle grain boundaries [40, 41]. After removing the casing from the CP-Ti billets, cracks were observed on the upper surface of the specimen after fourth pass. Therefore, in order to produce intact ultra-fine grain specimens without cracking, all bimetallic specimens were pressed up to the third pass at ambient temperature with the B_C route and all experimental tests were performed on un-ECAPed and ECAPed specimens in passes 1, 2 and 3. Figure (3) shows the bimetallic specimen before and after ECAP.

2.3 Experimental tests

- *Microstructural observations*

An Olympus BX60M optical microscope was used to examine changes in microstructure of CP-Ti before and after ECAP and to demonstrate grain refinement. Metallographic samples were cut from the middle of the billet and perpendicular to the pressing direction for microstructure analysis. Then, samples were ground using 100-2000 grit SiC papers and polished automatically to mirror-like finishes using 0.3 mm alumina particles. These samples were then etched to show grain boundaries by immersing them for up to 70 seconds in a solution containing distilled water, hydrofluoric acid, and hydrogen peroxide [H_2O (100 mL) + H_2O_2(35%) (5 mL) + HF (2 mL)]. The average grain size was determined from microstructural images by a line intercept method using MIP (Microstructural Image Processing) software according to ASTM E 112-96 standard.

- *Vickers hardness test*

The values of the Vickers micro-hardness (Hv) at the center of studied sections according to ASTM E 92 standard and using a Buehler micro-hardness tester with a load of 1 kgf and a dwell time of 15 s were measured. In order to achieve a high degree of accuracy, each reported micro-hardness value was at least the average of five separate measurements.

- *Corrosion test*

The corrosion test was performed to compare the corrosion resistance of Grade (2) CP-Ti in both un-ECAPed (CG) state and three-pass ECAPed state (UFG) in simulated body fluid (SBF). For this purpose, corrosion test specimens were prepared as cubes with a test surface of 5×5 mm^2 and then hot pressed in mounting resin to prepare the surface. Then, a hole with an approximate diameter of 3 mm was made from the back of the mount to the back surface of the sample, and a very small screw was inserted in that hole so that the end of the screw was in contact with the back of the mounted sample, without any mechanical pressure. A thin electrical wire was then connected to the screw head so that the sample could be in the current path between the electrode and the electrolyte. Subsequently, each of these two mounted specimens was ground and polished to a mirror-like finished surface before corrosion testing similar to surface preparation for the hardness test. After washing in distilled water, those were automatically washed for 30 minutes using an ultrasonic cleaning device (Whaledant/BioSonic UC100 Dental Ultrasonic Cleaner) in acetone liquid to remove any surface contamination [21]. In this study, simulated body fluid (SBF) was considered as the electrolyte. This liquid was made according to Kokubo method [42] with ionic composition similar to human body plasma

and in accordance with the conditions and compounds presented in Table (2). This liquid was used as a freshly prepared solution for each corrosion test. A three-electrode electrochemical cell was set up to perform the corrosion test and measure the corrosion rate by TAFEL extrapolation. These three electrodes, including working electrode (WE), reference electrode (RE) or saturated calomel electrode (SCE), and an auxiliary electrode (AE) or neutral or counter (CE), were connected to the Gill AC V5 automatic potentiostat device (Gill AC Version 5, ACM Instruments, UK) and the device was connected to its software environment on the computer. The potentiostat device controls the voltage between WE and RE and transmits it to the software environment.

In this study, the auxiliary electrode was made of platinum and has an area of 2 cm^2. The working electrode was connected to the screw attached to Ti sample via an electric current conductor wire. The area of studied polished CP-Ti is 25 mm^2, which is directly exposed to SBF solution. During the test, the temperature of the SBF solution was kept at 37±1°C to perform corrosion at temperatures close to normal human body temperature. By placing the Becher of the electrochemical cell in the temperature controlled bath, the temperature of the cell can be adjusted and kept constant at any time. A constant open circuit potential (OCP) was established between the sample and the reference electrode for 30 minutes to obtain the appropriate range of applied potentials for corrosion. Subsequently, the potentiodynamic technique was used to obtain the current density diagram (current per unit area) versus the potential or TAFEL polarization diagram [21].

The TAFEL test was performed in the voltage range of -800 mV to + 800 mV with a scan rate of 1 mV/s. The amount of corrosion current obtained by the TAFEL technique indicates the corrosion rate. So that, more corrosion current density indicates the higher corrosion rate or lower corrosion resistance. These tests were repeated three times for each sample in freshly prepared electrolyte and in each replication, the surfaces of samples prepared completely according to the mentioned conditions.

Figure (4) shows a real view of a three-electrode electrochemical cell. As is clear; the mounted specimen is suspended so that the surface of the titanium specimen is fully exposed to the electrolyte SBF solution. The thermometer is placed next to the three electrodes to instantly check the test temperature during the test period. The complete setup of the electrochemical test for determining the corrosion behavior of CP-Ti before (CG) and after applying 3 passes of ECAP (UFG) was also demonstrated in Figure (5).

Table 2 Reagents for preparing 1 litter of SBF with PH 7.4 [18]

Order	Reagent	Amount (g/l)
1	NaCl	7.996 g
2	$NaHCO_3$	0.350 g
3	KCl	0.224 g
4	$K_2HPO_43H_2O$	0.228 g
5	$MgCl_26H_2O$	0.305 g
6	1 M-HCl	40.0 ml
7	$CaCl_2$	0.278 g
8	Na_2SO_4	0.071 g
9	$(CH_2OH)_3CNH_2$	6.057 g

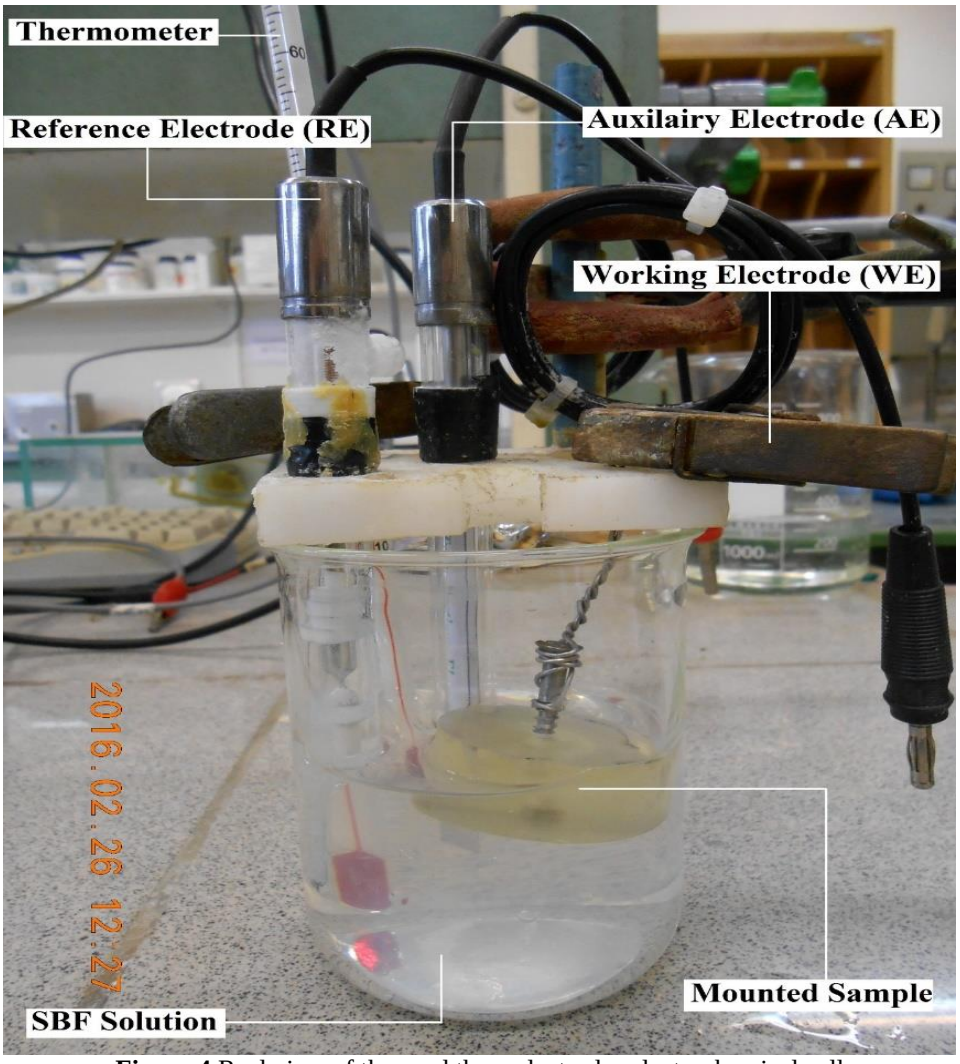

Figure 4 Real view of the used three electrodes electrochemical cell

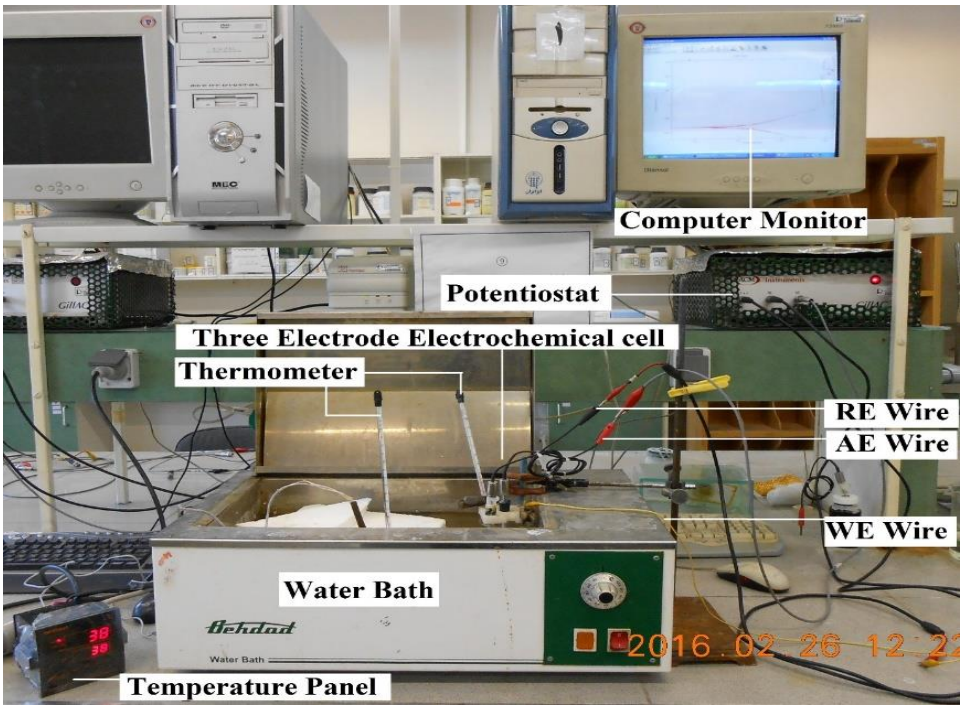

Figure 5 Real view of the three electrodes electrochemical cell setup used for corrosion testing

3 Results and discussion

3.1 Microstructure

Grade (2) CP-Ti microstructures obtained from an optical microscope, before and after ECAP process up to three passes, were shown in Figure (6). These microscopic images clearly show grain refinement and elongated microstructure due to cold severe plastic deformation. The average grain size decreased from 55 μm for initial annealed CP-Ti to 11, 3 and 0.65 μm after the first, second and third passes of introducing ECAP, respectively. As can be seen, the grains become smaller as the number of ECAP passes increases. After the first pass, the parallel shear bands consist of a high density of dislocation, more complex bands at the intersection of two different directions, and a high density of twins, parallel to the elongated structure, were generated. The development of low-angle grain boundaries to high-angle grain boundaries always occurs after the first pass of ECAP in metals with hexagonal closed pack (hcp) crystal lattice structures such as titanium [7, 43-45]. At higher passes, complex banded structures are formed and with increasing number of passes, coarse and elongated grains do not become more elongated, but a uniform microstructure is formed without the presence of banded structures [43, 44].

3.2 Hardness

Vickers microhardness of Grade (2) CP-Ti billets was measured before and after the ECAP process at BC route. These tests were performed at the cross-sectional surface of the ECAPed specimens after 1 to 3 passes. The results demonstrated that, Vickers microhardness from HV 153 for un-ECAPed specimen was enhanced to HV 193, HV 215 and HV 247 for specimens after applying 1, 2 and 3 passes of ECAP, respectively. It can be seen that, the microhardness of Grade (2) CP-Ti increased significantly after a single pass of ECAP process and increasing the pass number lead to improvement of hardness value. This result is due to grain refinement and microstructural evolution resulting from cold working imposed by ECAP [46, 47]. It can be expected that with increasing hardness due to the application of ECAP, the static strength of this material, such as tensile strength will also increase [48].

3. 3 Corrosion resistance in SBF

In this research, un-ECAPed (CG) and ECAPed up to 3 passes (UFG) CP-Ti were tested for corrosion at 37°C in a SBF electrolyte solution. By extracting the TAFEL curve, the corrosion current density ($\mu A/cm^2$), which represents the corrosion rate and consequently the corrosion resistance; was reported. Figure (7) shows the potential curve in terms of the logarithm of the corrosion current density, which indicates the corrosion rate by the TAFEL extrapolation method. The results that can be obtained from this diagram include anodic slope, cathodic slope and corrosion current density. These results were presented in Table (3). The anodic slope represents the linear slope of a branch of the curve that loses electrons and moves toward a positive potential, and the cathodic slope represents the linear slope of a branch of the curve that moves toward a negative potential with electrons receiving.

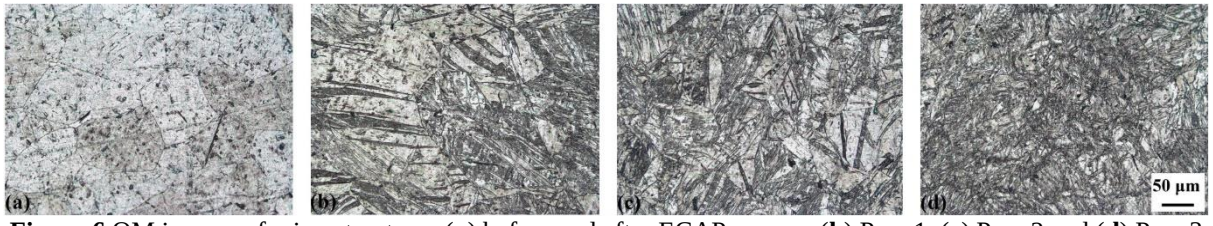

Figure 6 OM images of microstructures (**a**) before and after ECAP process (**b**) Pass 1, (**c**) Pass 2 and (**d**) Pass 3

The intersection point of these two linear slopes (cathodic and the anodic TAFEL slopes) that are true at least on one decade (10^{-n-1} to 10^{-n} , $n \epsilon N$) of logarithms of current intensity, introduces the corrosion current density. As is clear from the results; the amount of corrosion current density in CG state is 0.37 μA/cm^2 and in UFG state is 0.053 μA/cm^2. Therefore, it can be concluded that the corrosion resistance of CP-Ti after grain refining by the ECAP process has been increased approximately 7 times compared to the primary annealed CP-Ti.

Enhancement of the corrosion resistance of CP-Ti in UFG state relative to CG state can be attributed to an increase of passivation ability as a result of the rapid mechanical formation of a stable and strong passive oxide film of titanium dioxide (TiO_2) on the UFG surface relative to CG CP-Ti. CG corrosion in SBF is mainly due to the decomposition of the weak passive oxide film TiO_2 by Cl^- ions as a result of localized corrosion. Thus, it has been observed the failure of this film in some areas of the surface, has increased the pitting corrosion. But in the case of UFG, high-density grain boundaries help to increase the interfacial adherence of the passive oxide film. This is due to the oxide protrusions penetrating into the grain boundaries, similar to so-called oxide pegs in some ferrous alloys; which leads to a significant increase in corrosion resistance [21, 22]. Studies have also shown that the presence of more residual compressive stress at the UFG surface due to the introduction of the ECAP process, can help reduce the corrosion rate and thus improve corrosion resistance. In addition, it has been demonstrated that the presence of pressure around micro defects delays the local entry of hydrogen and reduces the possibility of hydrogen embrittlement and makes the rupture of the passive oxide film harder [21, 49].

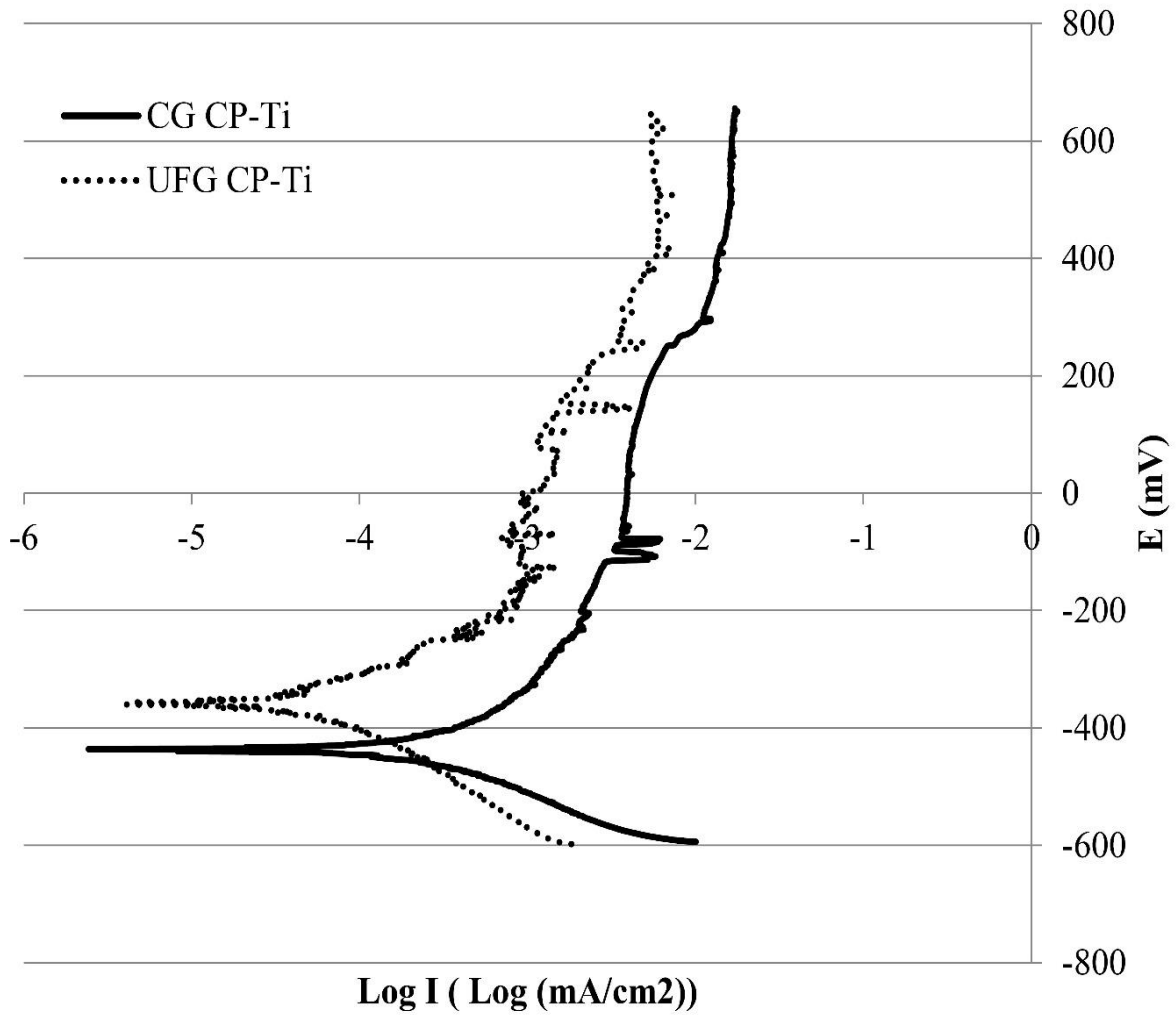

Figure 7 TAFEL extraction curve for CP-Ti in two states CG (Un-ECAPed) and UFG (After pass 3)

Table 3 Electrochemical properties of CP-Ti in two states CG (Un-ECAPed) and UFG (After pass 3)

Grade (2) CP-Ti	Corrosion Current Density (μA/cm^2)	Cathodic TAFEL Slope (mV/decade)	Anodic TAFEL Slope (mV/decade)
CG (Un-ECAPed)	0.370	-136	321
UFG (After Pass 3)	0.053	-164	193

On the other hand, the improvement of corrosion behavior in UFG state compared to CG state in SBF, in addition to grain size, is also attributed to changes in crystallographic texture [22, 27]. The increased density of crystalline defects on the surface of the ECAPed samples is responsible for this issue. The microstructural developments induced by this process predominantly influence the anodic reactions occurring on the metal surface. For the annealed sample, the surface initially exhibits fully active behavior during anodic polarization. For the 3-pass sample, the trend differs from the other samples. In this case, the conditions for the formation of a corrosion film are established. Additionally, the sample exhibits relatively active behavior, with continued polarization accompanied by an increase in anodic current density. An important point about this sample is that the anodic current density is lower than that of un-ECAPed samples. In other words, during the anodic polarization of the 3-pass ECAPed sample within this potential range, more favorable protection conditions may exist compared to other samples due to the products formed on the surface [31].

4 Conclusions

In this research, the ECAP process was applied at ambient temperature on commercially pure titanium (CP-Ti) for up to three passes and the primary annealed coarse grain (CG) structure was changed to ultra-fine grained structures (UFG). The study of microstructure, hardness and corrosion in simulated body fluid (SBF) was performed on this material before and after three passes of ECAP and the following results were obtained:

- The grain size decreased from 55 μm in annealed CG state, to 11, 3 and 0.65 μm after applying 1, 2 and 3 passes of ECAP, respectively. The results show that after applying three passes of ECAP process at ambient temperature in the channel of 135°, an ultra-fine grain microstructure with an average grain size of 650 nm can be achieved.
- The microVickers (Hv) hardness tests were conducted on CP-Ti before and after imposing the three passes of ECAP and the results showed that the Vickers hardness of this material increased from 153 Hv for the primary CG state to 193, 215 and 247 Hv after applying 1, 2, and 3 passes of ECAP, respectively. This indicates that the hardness of the material has increased significantly by applying the cold ECAP process.
- To determine the corrosion behavior of this material before and after applying the ECAP process, the TAFEL curve extraction was used and the corrosion current density, which represents the corrosion rate and consequently corrosion resistance, was reported. The amount of the corrosion current density was 0.37 μA/cm^2 before ECAP (CG) and 0.053 μA/cm^2 after the third pass of ECAP (UFG). Therefore, it was concluded that the corrosion resistance in the simulated body fluid after grain refinement by ECAP has increased almost seven times compared to the primary coarse grain pure titanium.

References

[1] M. Geetha, A. K. Singh, R. Asokamani, and A. K. Gogia, "Ti Based Biomaterials, the Ultimate Choice for Orthopaedic Implants–a Review", *Progress in Materials Science*, Vol. 54, No. 3, pp. 397-425, 2009, https://doi.org/10.1016/j.pmatsci.2008.06.004.

[2] H. J. Rack, and J. I. Qazi, "Titanium Alloys for Biomedical Applications", *Materials Science and Engineering: C*, Vol. 26, No. 8, pp. 1269-1277, 2006, https://doi.org/10.1016/j.msec.2005.08.032.

[3] P. S. Roodposhti, N. Farahbakhsh, A. Sarkar, and K. L. Murty, "Microstructural Approach to Equal Channel Angular Processing of Commercially Pure Titanium—A Review", *Transactions of Nonferrous Metals Society of China*, Vol. 25, No. 5, pp. 1353-1366, 2015, https://doi.org/10.1016/S1003-6326(15)63734-7.

[4] M. Bonyadi Manesh, N. Vatankhah, and F. Bonyadi Manesh, "Comparison of Microbiota in Zirconia and Titanium Implants: A Qualitative Systematic Review", *International Dental Journal*, Vol. 75, No. 1, 2024, https://doi.org/10.1016/j.identj.2024.08.001.

[5] S. Nag, R. Banerjee, and H. L. Fraser, "Microstructural Evolution and Strengthening Mechanisms in Ti–Nb–Zr–Ta, Ti–Mo–Zr–Fe and Ti–15Mo Biocompatible Alloys", *Materials Science and Engineering: C*, Vol. 25, No. 3, pp. 357-362, 2005, https://doi.org/10.1016/j.msec.2004.12.013.

[6] Y. J. Chen, Y. J. Li, J. C. Walmsley, S. Dumoulin, P. C. Skaret, and H. J. Roven, "Microstructure Evolution of Commercial Pure Titanium during Equal Channel Angular Pressing", *Materials Science and Engineering: A*, Vol. 527, No. 3, pp. 789-796, 2010, https://doi.org/10.1016/j.msea.2009.09.005.

[7] R. Z. Valiev, and T. G. Langdon, "Principles of Equal-channel Angular Pressing as a Processing Tool for Grain Refinement", *Progress in Materials Science*, Vol. 51, No. 7, pp. 881-981, 2006, https://doi.org/10.1016/j.pmatsci.2006.02.003.

[8] Z. Horita, T. Fujinami, and T. G. Langdon, "The Potential for Scaling ECAP: Effect of Sample Size on Grain Refinement and Mechanical Properties", *Materials Science and Engineering: A*, Vol. 318, No. 1-2, pp. 34-41, 2001, https://doi.org/10.1016/S0921-5093(01)01339-9.

[9] R. Z. Valiev, R. K. Islamgaliev, and I. V. Alexandrov, "Bulk Nanostructured Materials from Severe Plastic Deformation", *Progress in Materials Science*, Vol. 45, No. 2, pp. 103-189, 2000, https://doi.org/10.1016/S0079-6425(99)00007-9.

[10] H. Maleki Ghaleh, K. Hajizadeh, A. Hadjizadeh, M. S. Shakeri, S. G. Alamdari, S. Masoudfar, E. Aghaie, M. Javidi, J. Zdunek, and K. J. Kurzydlowski, "Electrochemical and Cellular Behavior of Ultrafine-grained Titanium In Vitro", *Materials Science and Engineering: C*, Vol. 39, pp. 299-304, 2014, https://doi.org/10.1016/j.msec.2014.03.001.

[11] T. N. Kim, A. Balakrishnan, B. C. Lee, W. S. Kim, K. Smetana, J. K. Park, and B. B. Panigrahi, "In Vitro Biocompatibility of Equal Channel Angular Processed (ECAP) Titanium", *Biomedical Materials*, Vol. 2, No. 3, pp. S 117-S 120, 2007, https://doi.org/10.1088/1748-6041/2/3/s06.

[12] A. Thirugnanam, T. S. S. Kumar, and U. Chakkingal, "Tailoring the Bioactivity of Commercially Pure Titanium by Grain Refinement using Groove Pressing", *Materials Science and Engineering: C*, Vol. 30, No. 1, pp. 203-208, 2010, https://doi.org/10.1016/j.msec.2009.10.002.

[13] L. Le Guéhennec, A. Soueidan, P. Layrolle, and Y. Amouriq, "Surface Treatments of Titanium Dental Implants for Rapid Osseointegration", *Dental Materials*, Vol. 23, No. 7, pp. 844-854, 2007, https://doi.org/10.1016/j.dental.2006.06.025.

[14] S. Faghihi, A. P. Zhilyaev, J. A. Szpunar, F. Azari, H. Vali, and M. Tabrizian, "Nanostructuring of a Titanium Material by High-pressure Torsion Improves Pre-osteoblast Attachment", *Advanced Materials*, Vol. 19, No. 8, pp. 1069-1073, 2007, https://doi.org/10.1002/adma.200602276.

[15] L. Ostrovska, L. Vistejnova, J. Dzugan, P. Slama, T. Kubina, E. Ukraintsev, D. Kubies, M. Kralickova, and M. H. Kalbacova, "Biological Evaluation of Ultra-fine Titanium with Improved Mechanical Strength for Dental Implant Engineering", *Journal of Materials Science*, Vol. 51, No. 6, pp. 3097-3110, 2016, https://doi.org/10.1007/s10853-015-9619-3.

[16] M. Abbasi, F. Ahmadi, and M. Farzin, "Production of Ultrafine-grained Titanium with Suitable Properties for Dental Implant Applications by RS-ECAP Process", *Metals and Materials International*, Vol. 27, No. 4, pp. 705-716, 2021, https://doi.org/10.1007/s12540-020-00796-5.

[17] R. Chen, Y. Yao, J. Yong, S. Zhu, X. Xu, and N. Dai, "Pulsed Laser Surface Texturing Enhancing Corrosion Resistance of Rare-earth WE43 Magnesium Alloys in Simulated Body Fluid Environment", *Journal of Alloys and Compounds*, pp. 176197, 2024, https://doi.org/10.1016/j.jallcom.2024.176197.

[18] P. N. Chavan, M. M. Bahir, R. U. Mene, M. P. Mahabole, and R. S. Khairnar, "Study of Nanobiomaterial Hydroxyapatite in Simulated Body Fluid: Formation and Growth of Apatite", *Materials Science and Engineering: B*, Vol. 168, No. 1, pp. 224-230, 2010, https://doi.org/10.1016/j.mseb.2009.11.012.

[19] A. A. Mendes Filho, C. A. Rovere, S. E. Kuri, V. L. Sordi, and M. Ferrante, "A General Study of Commercially Pure Ti Subjected to Severe Plastic Deformation: Microstructure, Strength and Corrosion Resistance", *Revista Matéria (Rio de Janeiro)*, Vol. 15, No. 2, pp. 254-259, 2010, https://doi.org/10.1590/S1517-70762010000200024.

[20] A. A. Mendes Filho, V. L. Sordi, and M. Ferrante, "The Effects of Severe Plastic Deformation on Some Properties Relevant to Ti Implants", *Materials Research*, Vol. 15, No. 1, pp. 27-31, 2012, https://doi.org/10.1590/S1516-14392011005000102.

[21] A. Balakrishnan, B. C. Lee, T. N. Kim, and B. B. Panigrahi, "Corrosion Behaviour of Ultra Fine Grained Titanium in Simulated Body Fluid for Implant Application", *Trends in Biomaterials & Artificial Organs*, Vol. 22, No. 1, pp. 58-64, 2008, https://www.semanticscholar.org/paper/Corrosion-Behaviour-of-Ultra-Fine-Grained-Titanium-Balakrishnan-Lee/bc1a3c58e7c2f1a7ef37750e4db3ff1ef75de7a4.

[22] M. Hoseini, A. Shahryari, S. Omanovic, and J. A. Szpunar, "Comparative Effect of Grain Size and Texture on the Corrosion Behaviour of Commercially Pure Titanium Processed by Equal Channel Angular Pressing", *Corrosion Science*, Vol. 51, No. 12, pp. 3064-3067, 2009, https://doi.org/10.1016/j.corsci.2009.08.017.

[23] Y. Dong, X. Li, Z. Yu, I. Alexandrov, H. Chang, and L. Zhou, "Corrosion Resistance of Ultrafine-grained Titanium Alloys in Different Corrosive Environments", in *MATEC Web of Conferences, The 14th World Conference on Titanium (Ti 2019)*, June 10, 2019, Nantes, France, Vol. 321, p. 06001, EDP Sciences, https://doi.org/10.1051/matecconf/202032106001.

[24] V. N. Chuvil'deev, A. A. Murashov, A. V. Nokhrin, N. N. Berendeev, C. V. Likhnitskii, A. N. Sysoev, N. V. Melekhin, K. A. Rubtsova, A. M. Bakmetyev, and P. V. Tryaev, "Effect of Annealing on the Corrosion-fatigue Strength and Hot Salt Corrosion Resistance of Fine-grained Titanium near-a Alloy Ti-5Al-2V Obtained by Rotary Swaging", *Journal of Alloys and Compounds*, Vol. 1003, pp. 175612, 2024, https://doi.org/10.1016/j.jallcom.2024.175612.

[25] H. S. Kim, and W. J. Kim, "Annealing Effects on the Corrosion Resistance of Ultrafine-grained Pure Titanium", *Corrosion Science*, Vol. 89, pp. 331-337, 2014, https://doi.org/10.1016/j.corsci.2014.08.017.

[26] M. Otadi, E. Borhani, and S. Faghihi, "Combined Bulk Nanostructuring and Surface Modifications of Titanium Substrate for Improved Corrosion Behavior", *Surface and Coatings Technology*, Vol. 493, pp. 131229, 2024, https://doi.org/10.1016/j.surfcoat.2024.131229.

[27] N. P. Gurao, G. Manivasagam, P. Govindaraj, R. Asokamani, and S. Suwas, "Effect of Texture and Grain Size on Bio-corrosion Response of Ultrafine-grained Titanium", *Metallurgical and Materials Transactions A*, Vol. 44, No. 12, pp. 5602-5610, 2013, https://doi.org/10.1007/s11661-013-1910-9.

[28] C. Y. Zheng, F. L. Nie, Y. F. Zheng, Y. Cheng, S. C. Wei, and R. Z. Valiev, "Enhanced in Vitro Biocompatibility of Ultrafine-grained Titanium with Hierarchical Porous Surface", *Applied Surface Science*, Vol. 257, No. 13, pp. 5634-5640, 2011, https://doi.org/10.1016/j.apsusc.2011.01.062.

[29] M. M. Nair, and S. Swaroop, "Influence of Oxide Layer Developed by Laser Shock Peening on Biocorrosion Response of Ti-6Al-7Nb in Simulated Body Fluid", *Surface and Coatings Technology*, Vol. 483, pp. 130795, 2024, https://doi.org/10.1016/j.surfcoat.2024.130795.

[30] A. Balyanov, J. Kutnyakova, N. A. Amirkhanova, V. V. Stolyarov, R. Z. Valiev, X. Z. Liao, Y. H. Zhao, Y. B. Jiang, H. F. Xu, and T. C. Lowe, "Corrosion Resistance of Ultra Fine-grained Ti", *Scripta Materialia*, Vol. 51, No. 3, pp. 225-229, 2004, https://doi.org/10.1016/j.scriptamat.2004.04.011.

[31] F. Fakheri, S. Pour-Ali, R. Tavangar, and R. Naseri, "Effect of Ultrasonic Assisted-ECAP Processing on the Microstructure, Mechanical Properties, and Fluoride-induced Corrosion Performance of Pure Titanium", *Materials Today Communications*, Vol. 40, pp. 109863, 2024, https://doi.org/10.1016/j.mtcomm.2024.109863.

[32] X. Y. Liu, X. C. Zhao, X. R. Yang, C. Xie, and G. J. Wang, "Compression Deformation Behaviours of Ultrafine and Coarse Grained Commercially Pure Titanium", *Materials Science and Technology*, Vol. 29, No. 4, pp. 474-479, 2013, https://doi.org/10.1179/1743284712Y.0000000164.

[33] A. Bahmani, and K. S. Shin, "*Effects of Severe Plastic Deformation on Mechanical Properties and Corrosion Behavior of Magnesium Alloys*", (Conference Paper - Part of the Book Series: The Minerals, Metals & Materials Series (MMMS)), Springer, Chamm, pp. 369–371, 2018, https://doi.org/10.1007/978-3-319-72332-7_57.

[34] M. H. Shaeri, F. Djavanroodi, M. Sedighi, S. Ahmadi, M. T. Salehi, and S. H. Seyyedein, "Effect of Copper Tube Casing on Strain Distribution and Mechanical Properties of Al-7075 Alloy Processed by Equal Channel Angular Pressing", *The Journal of Strain Analysis for Engineering Design*, Vol. 48, No. 8, pp. 512-521, 2013, https://doi.org/10.1177/0309324713498234.

[35] F. Djavanroodi, M. Daneshtalab, and M. Ebrahimi, "A Novel Technique to Increase Strain Distribution Homogeneity for ECAPed Materials", *Materials Science and Engineering: A*, Vol. 535, pp. 115-121, 2012, https://doi.org/10.1016/j.msea.2011.12.050.

[36] R. Naseri, M. Kadkhodayan, and M. Shariati, "An Experimental Investigation of Casing Effect on Mechanical Properties of Billet in ECAP Process", *The International Journal of Advanced Manufacturing Technology*, pp. 1-14, 2016, https://doi.org/10.1007/s00170-016-9658-1.

[37] M. Ebrahimi, M. H. Shaeri, R. Naseri, and C. Gode, "Equal Channel Angular Extrusion for Tube Configuration of Al-Zn-Mg-Cu Alloy", *Materials Science and Engineering: A*, Vol. 731, pp. 569-576, 2018, https://doi.org/10.1016/j.msea.2018.06.080.

[38] W. J. Kim, C. Y. Hyun, and H. K. Kim, "Fatigue Strength of Ultrafine-grained Pure Ti after Severe Plastic Deformation", *Scripta Materialia*, Vol. 54, No. 10, pp. 1745-1750, 2006, https://doi.org/10.1016/j.scriptamat.2006.01.042.

[39] S. Zhang, Y. C. Wang, A. P. Zhilyaev, E. Korznikova, S. Li, G. I. Raab, and T. G. Langdon, "Effect of Grain Size on Compressive Behaviour of Titanium at Different Strain Rates", *Materials Science and Engineering: A*, Vol. 645, pp. 311-317, 2015, https://doi.org/10.1016/j.msea.2015.08.031.

[40] V. V. Stolyarov, Y. T. Zhu, I. V. Alexandrov, T. C. Lowe, and R. Z. Valiev, "Influence of ECAP Routes on the Microstructure and Properties of Pure Ti", *Materials Science and Engineering: A*, Vol. 299, No. 1, pp. 59-67, 2001, https://doi.org/10.1016/S0921-5093(00)01411-8.

[41] S. N. Alhajeri, N. Gao, and T. G. Langdon, "Hardness Homogeneity on Longitudinal and Transverse Sections of an Aluminum Alloy Processed by ECAP", *Materials Science and Engineering: A*, Vol. 528, No. 10, pp. 3833-3840, 2011, https://doi.org/10.1016/j.msea.2011.01.074.

[42] T. Kokubo, H. Kushitani, S. Sakka, T. Kitsugi, and T. Yamamuro, "Solutions Able to Reproduce in Vivo Surface-structure Changes in Bioactive Glass-ceramic a-W3", *Journal of Biomedical Materials Research*, Vol. 24, No. 6, pp. 721-734, 1990, https://doi.org/10.1002/jbm.820240607.

[43] X. Zhao, X. Yang, X. Liu, C. T. Wang, Y. Huang, and T. G. Langdon, "Processing of Commercial Purity Titanium by ECAP using a 90 Degrees Die at Room Temperature",

Materials Science and Engineering: A, Vol. 607, pp. 482-489, 2014, https://doi.org/10.1016/j.msea.2014.04.014.

[44] X. Zhao, X. Yang, X. Liu, X. Wang, and T. G. Langdon, "The Processing of Pure Titanium through Multiple Passes of ECAP at Room Temperature", *Materials Science and Engineering: A*, Vol. 527, No. 23, pp. 6335-6339, 2010, https://doi.org/10.1016/j.msea.2010.06.049.

[45] Y. Li, H. P. Ng, H. D. Jung, H. E. Kim, and Y. Estrin, "Enhancement of Mechanical Properties of Grade 4 Titanium by Equal Channel Angular Pressing with Billet Encapsulation", *Materials Letters*, Vol. 114, pp. 144-147, 2014, https://doi.org/10.1016/j.matlet.2013.09.118.

[46] R. Naseri, M. Kadkhodayan, and M. Shariati, "Static Mechanical Properties and Ductility of Biomedical Ultrafine-grained Commercially Pure Titanium Produced by ECAP Process", *Transactions of Nonferrous Metals Society of China*, Vol. 27, No. 9, pp. 1964-1975, 2017, https://doi.org/10.1016/S1003-6326(17)60221-8.

[47] R. Naseri, H. Hiradfar, M. Shariati, and M. Kadkhodayan, "A Comparison of Axial Fatigue Strength of Coarse and Ultrafine Grain Commercially Pure Titanium Produced by ECAP", *Archives of Civil and Mechanical Engineering*, Vol. 18, No. 3, pp. 755-767, 2018, https://doi.org/10.1016/j.acme.2017.12.005.

[48] X. Zhao, W. Fu, X. Yang, and T. G. Langdon, "Microstructure and Properties of Pure Titanium Processed by Equal-channel Angular Pressing at Room Temperature", *Scripta Materialia*, Vol. 59, No. 5, pp. 542-545, 2008, https://doi.org/10.1016/j.scriptamat.2008.05.001.

[49] X. Liu, and G. S. Frankel, "Effects of Compressive Stress on Localized Corrosion in AA2024-T3", *Corrosion Science*, Vol. 48, No. 10, pp. 3309-3329, 2006, https://doi.org/10.1016/j.corsci.2005.12.003.